Synthesis and Characterization of Poly(L-lactide-co-ε-caprolactone) Copolymers: Effects of Stannous Octoate Initiator and Diethylene Glycol Coinitiator Concentrations

Yodthong Baimark and Robert Molloy*

Biomedical Polymers Technology Unit, Department of Chemistry, Faculty of Science, Chiang Mai University, Chiang Mai 50200, Thailand.

* Corresponding author, E-mail: robert@chiangmai.ac.th

ABSTRACT: A series of approximately 50:50 mol % poly(L-lactide-*co*-ε-caprolactone) copolymers were synthesized by bulk copolymerization of L-lactide (LL) and ε-caprolactone (CL) using stannous octoate ($Sn(Oct)_2$) and diethylene glycol (DEG) as the initiating system. The resulting P(LL-*co*-CL) copolymers were characterized by various analytical techniques including dilute-solution viscometry, GPC, $^1H/^{13}C$ NMR and DSC. It was found that both the $Sn(Oct)_2$ and DEG concentrations exerted important but different effects on the molecular weight (average and distribution), chain microstructure and temperature transitions of the copolymer formed. Whereas the $Sn(Oct)_2$ initiator mainly affected the molecular weight distribution and comonomer sequencing, the DEG coinitiator was more influential on the average molecular weight. The results are discussed in the light of current theories of the coordination-insertion mechanism of cyclic ester ring-opening polymerization.

KEYWORDS: L-lactide, ε-caprolactone, poly(L-lactide-*co*-ε-caprolactone), biodegradable polyesters.

INTRODUCTION

During the past 3 decades, research interest in random copolymers of L-lactide (LL) and ε-caprolactone (CL) has increased steadily as their potential in a wide range of biomedical applications has been realized. These applications have so far included biodegradable controlled-release drug delivery systems,[1,2] monofilament surgical sutures[3,4] and, most recently, absorbable nerve guides.[5] By varying the copolymer composition, monomer sequencing and molecular weight, the copolymer properties can be tailored to meet the specific requirements of each particular application. The copolymers have been shown to be both biocompatible and biodegradable. Biodegradation proceeds via simple hydrolysis (random chain scission) leading to progressively lower molecular weight fragments. In the case of LL-rich fragments, hydrolysis usually continues unabated until L-lactic acid is formed. However, CL-rich fragments tend to be taken up in the final stage by macrophages and giant cells and degraded within these cells by enzymes before eventually yielding ε-hydroxycaproic acid. Both L-lactic acid and ε-hydroxycaproic acid are either metabolizable or excretable from the human body without any adverse toxicological effects.

Previous studies of the synthesis of poly(L-lactide-*co*-ε-caprolactone), P(LL-*co*-CL), copolymers revealed the sensitivity of copolymer microstructure and molecular weight to the copolymerization conditions used.[6-9] Amongst these conditions, the choice of initiating system was particularly influential. Grijpma and co-workers[6,7] studied the effects of temperature and time and demonstrated the increasing importance of transesterification reactions as both temperature and time increased. Microstructural characterization of P(LL-*co*-CL) random copolymers, both in terms of their monomer sequencing and average monomer block length, has been described by several workers using ^{13}C NMR as the main analytical technique.[8,10-11] Since the two monomer reactivity ratios are quite different[7,11], r_1 (LL) > r_2 (CL), tapered copolymers with some blocky character tend to be formed. However, transesterification, depending on the extent to which it occurs, tends to randomize the monomer sequencing.

Much of this previous work has concentrated on the synthesis and characterization of the copolymers formed. In parallel, a protracted debate about the exact nature of the underlying coordination-insertion mechanism of cyclic ester polymerization has been

conducted in the literature, as recently reviewed by Albertsson and Varma.[12] While these previous studies have clearly defined the central role which the initiating system (initiator-coinitiator) plays in controlling both the rate and polymer molecular weight in homopolymerization, much less attention has been paid to its influence on the chain microstructure in copolymerization. In view of the importance of microstructural control to the tailoring of copolymer properties, this present paper now focusses in more detail on the effects of the initiator-coinitiator concentrations and their ratio on the outcome of a random LL-CL copolymerization. The initiator-coinitiator combination chosen for this study was stannous octoate (Sn(Oct)$_2$)-diethylene glycol (DEG), a combination generally accepted for use where the polymer product is to be employed in a biomedical application. The results are discussed in the light of the latest mechanistic theories.

MATERIALS AND METHODS

Materials

L(-)-lactide monomer, hereafter referred to as simply L-lactide, was synthesized from L(+)-lactic acid (Fluka) and purified by repeated recrystallization from distilled ethyl acetate until a mol % purity (DSC) of at least 99.9 % was obtained. ε-Caprolactone (Fluka) monomer was purified by fractional distillation over calcium hydride under reduced pressure and stored over molecular sieves in a refrigerator.

The stannous octoate (Sigma) initiator, systematic name : tin(II) bis(2-ethylhexanoate), and the diethylene
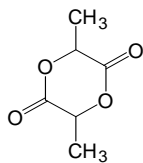

L(-)-lactide
LL
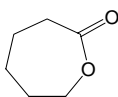
ε-caprolactone
CL

glycol (Fluka) coinitiator were also purified by fractional distillation under reduced pressure and stored over molecular sieves at room temperature. Ethyl acetate and toluene solvents, used for recrystallizing L-lactide and dissolving Sn(Oct)$_2$ respectively, were each purified by fractional distillation at normal pressure and stored over molecular sieves.

stannous octoate
Sn(Oct)$_2$

diethylene glycol
DEG
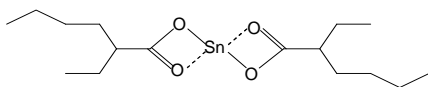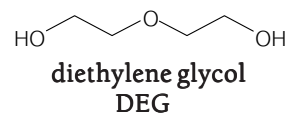
Analytical Methods

The intrinsic viscosity, $[\eta]$, of each copolymer was determined from flow-time measurements on a dilution series of solutions in chloroform as solvent at 30 °C using a Schott-Geräte AVS300 Automatic Viscosity Measuring System. The number-average molecular weight, M_n, and polydispersity, PD, were determined by gel permeation chromatography (GPC) using a Waters 150-CV GPC equipped with an Ultrastyragel® column operating at 30 °C and employing universal calibration. Chloroform was again used as the solvent at a flow rate of 1 ml min^{-1}.

Copolymer composition and monomer sequencing were characterized by a combination of high-resolution 300 MHz ^{1}H and 75 MHz ^{13}C nuclear magnetic resonance (NMR) spectrometry using a Bruker Avance DPX 300 ^{1}H/^{13}C NMR Spectrometer. Spectra were obtained from copolymer solutions in deuterated chloroform (CDCl$_3$) at room temperature.

Thermal analysis was carried out by means of differential scanning calorimetry (DSC) using a Mettler Toledo DSC822. Copolymer samples of 5-10 mg in weight were heated at 10 °C min^{-1} under a nitrogen atmosphere over the temperature range -70 to 200 °C in order to observe both the glass transition, Tg, and crystalline melting, Tm, temperatures. Prior to DSC analysis, the samples were stored in a vacuum desiccator at room temperature for at least 1 month in order to allow for any crystallization to take place, as had been previously reported.[13]

Copolymerizations

All copolymerizations were carried out in bulk at 140 °C under a dry nitrogen atmosphere. Scrupulous attention was paid to the purities of the reagents and the dryness of the apparatus. Even trace amounts of moisture and/or other hydroxyl-containing impurities (e.g., L-lactic acid and ε-hydroxycaproic acid impurities in the monomers) can influence the molecular weight of the final product via their possible roles as either coinitiators or hydrolysis/alcoholysis agents.

In the first set of experiments (Copolymer Nos. 1-5), the stannous octoate initiator concentration, [Sn(Oct)$_2$], was kept constant at 0.02 mol % relative to the total monomer concentration, [LL] + [CL] = [M], and the diethylene glycol coinitiator concentration, [DEG], varied over the range 0.16-0.80 mol %, i.e.

[M]/[Sn(Oct)$_2$]	=	5000
[M]/[DEG]	=	125-625
[DEG]/[Sn(Oct)$_2$]	=	8-40

Table 1. Effects of the Sn(Oct)$_2$ initiator and DEG coinitiator concentrations on the molecular weight characteristics of the copolymers formed.

Copolymer No.	Time (hrs)	M/DEG [a]	M/Sn [a]	[η] [b](dl/g)	$\overline{M}_n$ [c]	PD [d]
1	24	125.0	5,000	0.43	15,900	1.84
2	24	156.3	5,000	0.51	18,100	1.79
3	24	250.0	5,000	0.62	33,800	1.79
4	24	312.5	5,000	0.81	37,100	1.81
5	24	625.0	5,000	1.32	85,300	1.78
6	48	250.0	5,000	0.74	31,700	2.00
7	48	250.0	10,000	0.76	33,100	1.85
8	48	250.0	20,000	0.78	33,300	1.50

[a] M/DEG = [M]/[DEG] mole ratio; M/Sn = [M]/[Sn(Oct)$_2$] mole ratio; where [M] = [LL] + [CL] = total moles of comonomers
[b] measured in chloroform as solvent at 30 °C

[c] $\overline{M}_n$ value from GPC

[d] PD = polydispersity from GPC

In the second set of experiments (Copolymer Nos. 6-8), the [DEG] was kept constant at 0.40 mol % and the [Sn(Oct)$_2$] varied over the range 0.005-0.02 mol %, giving the ratios

[M]/[DEG]	=	250
[M]/[Sn(Oct)$_2$]	=	5000-20000
[DEG]/[Sn(Oct)$_2$]	=	20-80

These [Sn(Oct)$_2$] and [DEG] concentration ranges and ratios were chosen so as to encompass those which have been commonly reported in the literature in recent years for this and other similar initiating systems. For convenience and accuracy in weighing, Sn(Oct)$_2$ was prepared as a 0.8 M solution in dry toluene. Copolymerization temperature and times were based on past experience, the main considerations being to maximize conversion and molecular weight while minimizing the effects of transesterification. Consequently, a temperature of 140 °C was employed for all copolymerizations but the time depended on the rate of reaction which, in turn, appeared to be controlled mainly by the [Sn(Oct)$_2$]. Thus, for a [Sn(Oct)$_2$] = 0.02 mol %, a reaction time of 24 hrs was found to be sufficient, but for a [Sn(Oct)$_2$] < 0.02 mol %, a longer time of 48 hrs was needed to achieve a similar result.

At the end of each synthesis, the copolymer product was cut up into small pieces and dried to constant weight in a vacuum oven at 80 °C. Finally, it was stored in a vacuum desiccator at room temperature.

RESULTS AND DISCUSSION

Copolymer Characterization

Molecular weight characterization was carried out by means of a combination of dilute-solution viscometry and gel permeation chromatography (GPC).

Chloroform was used as the solvent at 30 °C in both techniques so that the equivalent copolymer-solvent interactions in solution would enable the results to be compared and, where possible, correlated. As seen in Table 1, the variations in the intrinsic viscosity, [η], values from viscometry are indeed consistent with those in the number-average molecular weights, $\overline{M}_n$, from GPC. This consistency substantiates the observed trends. All of the copolymers gave similar unimodal GPC molecular weight distributions, an example of which is shown in Fig 1 for Copolymer No. 1.

Copolymer compositions were determined from the ^{1}H NMR spectra by taking the ratio of the peak areas corresponding to the LL methine protons at δ = 5.0-5.3 ppm and the CL ϵ-methylene protons at δ = 3.9-4.2 ppm. The ^{1}H NMR spectrum of Copolymer No. 1 shown in Fig 2 is typical of those obtained. The calculated compositions (LL:CL mol %) in Table 2 are
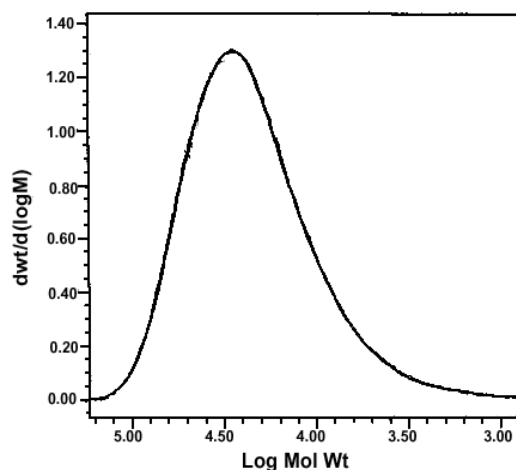
Fig 1. GPC molecular weight distribution curve for Copolymer No. 1.

Table 2. Effects of the Sn(Oct)$_2$ initiator and DEG coinitiator concentrations on the microstructural and thermal characteristics of the copolymers formed.

| Copolymer No.[a]	Composition [b] (LL : CL)	$\overline{L}_{LL}$ [c]	$\overline{L}_C$ [c]	T_g [d] (°C)	T_m [d] (°C)
1	48 : 52	3.2	2.8	-24	75
2	48 : 52	3.9	2.8	-37	41, 94
3	49 : 51	3.9	2.9	-35	42, 102
4	49 : 51	4.2	2.8	-37	42, 103
5	49 : 51	4.9	3.2	-36	42, 109
6	49 : 51	3.2	2.4	-21	39, 69
7	49 : 51	3.7	2.7	-27	42, 95
8	48 : 52	4.2	3.0	-30	41, 97

[a] conditions of synthesis as given in Table 1
[b] from the ^{1}H NMR spectrum; LL : CL (mol %)
[c] calculated from equations (1) and (2)
[d] from the DSC curve; T_g (mid-point), T_m (peaks)

all seen to be within 2% of the initial LL:CL = 50:50 comonomer feeds, as would be expected, since the copolymerizations were taken to near-quantitative conversion. The percent conversions after vacuum drying of the copolymers to constant weight were all in excess of 95 %.
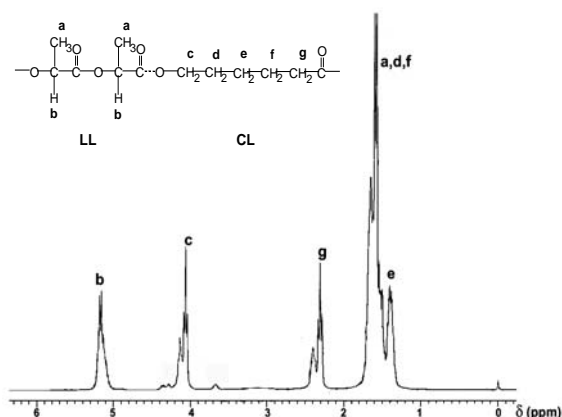

Fig 2. 300 MHz ^{1}H NMR spectrum of Copolymer No. 1 in CDCl$_3$ as solvent at room temperature.
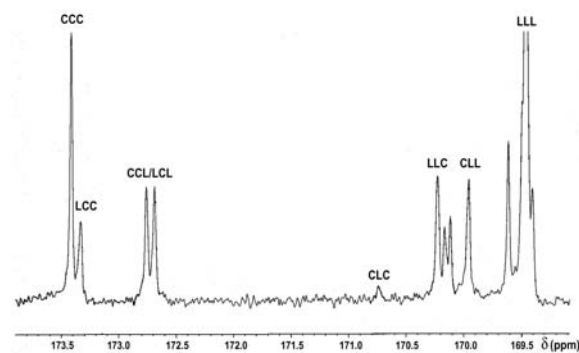
Fig 3. Expanded carbonyl region of the 75 MHz ^{13}C NMR spectrum of Copolymer No. 6 in CDCl$_3$ as solvent at room temperature.

Monomer sequencing in the copolymers was characterized from the ^{13}C NMR spectra, specifically from the expanded carbonyl carbon (C=O) region from $\delta = 169$-174 ppm. A typical example is shown in Fig 3 for Copolymer No. 6. The various peaks can be assigned to the C=O carbons of the middle units of various triad sequences, as labelled in Fig 3. For example, the small peak appearing at about 170.7 ppm corresponds to the CLC triad
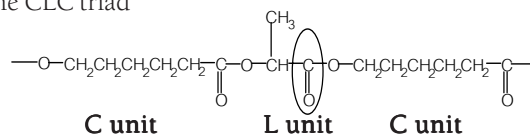
and is particularly interesting since a half-lactide (L) unit between two caprolactone (C) units can only occur via transesterification. The relative intensity of this CLC peak therefore provides some qualitative indication of the extent to which transesterification of the lactide units takes place.

(NOTE: It should be mentioned here that, whereas LL and CL are the common abbreviations for the L-lactide and ε-caprolactone monomer units in the copolymer's structural formula, the abbreviations commonly used for designating triad sequences are simply L and C. In these designations, L refers to only a half-lactide unit, -O-CH(CH$_3$)-CO-, in order to take account of their occurrence due to the cleavage of lactide monomer units by transesterification.)

A more quantitative approach is possible through the use of equations (1) and (2) which allow for calculation of the average monomer block lengths, $\overline{L}_{LL}$ and $\overline{L}_C$, of the respective monomer units from the triad peak intensities (I).[11] The various triad peaks which are referred to in these two equations are labelled in Fig 3.

$$\overline{L}_{LL} = \frac{1}{2}\left[\frac{l_{LLL}+(l_{LLC}+l_{CLL})/2}{(l_{LLC}+l_{CLL})/2+l_{CLC}}+1\right] \qquad (1)$$

$$\bar{L}_C = \frac{l_{CCC} + l_{LCC}}{l_{CCL} + l_{LCL}} + 1 \qquad (2)$$

The $\bar{L}_{LL}$ and $\bar{L}_C$ values for the copolymers are given in Table 2. Varying mainly within the range of 2-5, these values are consistent with a tapered monomer sequencing, bearing in mind that they will have been decreased to some extent during the course of the copolymerization by the randomizing effect of transesterification. The higher $\bar{L}_{LL}$ values reflect the higher reactivity ratio of L-lactide which, in microstructural terms, manifests itself as longer but fewer LL sequences than C sequences within the copolymer chain.

Thermal analysis of the copolymers was carried out by means of differential scanning calorimetry (DSC). To enable them to be compared, all of the copolymer samples had identical thermal histories. As shown in Figs 4 and 5, the DSC curves obtained each exhibit a
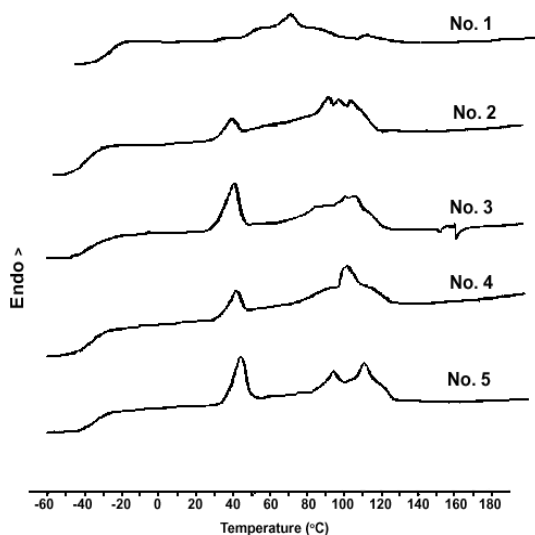
Fig 4. DSC thermograms of Copolymer Nos. 1→5 (as indicated) synthesized at constant [Sn(Oct)$_2$] and decreasing [DEG]. (Heating rate = 10 ^{o}C min^{-1}).
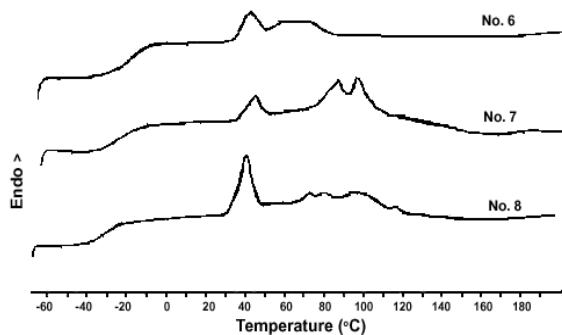
Fig 5. DSC thermograms of Copolymer Nos. 6→8 (as indicated) synthesized at constant [DEG] and decreasing [Sn(Oct)$_2$]. (Heating rate = 10 ^{o}C min^{-1}).

clear, well defined glass transition over the range of -40 to -20 ^{o}C but a very broad melting transition from 30-130 ^{o}C. Furthermore, the melting transition shows evidence of two distinct melting ranges, the lower narrower one at 30-50 ^{o}C corresponding to caprolactone-rich crystalline domains and the higher broader one at 60-130 ^{o}C corresponding to domains rich in L-lactide. These observations, together with the fact that these copolymers can crystallize at all despite their near 50:50 compositions, are further indications of the tapered character of the copolymer chain microstructures.

The glass transition, T_g, and melting peak, T_m, temperatures are given in Table 2. It is interesting to compare the T_g values with that which can be calculated from the Fox Equation (3) for a random copolymer of known composition:
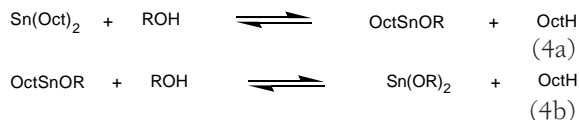
$$\frac{w_{LL}}{T_{g_{LL}}} + \frac{w_{CL}}{T_{g_{CL}}} = \frac{1}{T_{g_{LL-CL}}} \qquad (3)$$

where w_{LL} and w_{CL} are the respective weight fractions of the LL and CL monomer units in the copolymer while $T_{g_{LL}}$ and $T_{g_{CL}}$ are the respective T_g (K) values of the PLL and PCL homopolymers. For a 49:51 mol % LL:CL copolymer composition, as in Table 2, $w_{LL} = 0.55$ and $w_{CL} = 0.45$. Substituting these and the reference T_g values[14] of $T_{g_{LL}} = 65$ ^{o}C (338 K) and $T_{g_{CL}} = -60$ ^{o}C (213 K) into equation (3) yields a predicted random copolymer T_g of -6 ^{o}C. The fact that most of the experimental values in Table 2 are more than 20 ^{o}C lower than this predicted value is further evidence of the deviation from a random monomer sequencing. The experimental values also suggest that, as they are considerably closer to the T_g of PCL than PLL, the amorphous regions of the copolymers are proportionately richer in CL units.

Finally, it is also interesting to compare Copolymer Nos. 3 and 6 across the two series in Table 1, since they were each synthesized using the same [Sn(Oct)$_2$] and [DEG] concentrations but for different reaction times (24 and 48 hrs respectively). The differences in their properties, for example the slightly higher PD (Table 1) and lower $\bar{L}_{LL}$ and $\bar{L}_C$ (Table 2) values for Copolymer No. 6, can be largely attributed to increasing transesterification as the reaction time is increased.

Mechanistic Considerations

After much discussion in recent years, it is now becoming increasingly accepted that, when Sn(Oct)$_2$ is used in conjunction with an alcohol, ROH, as the initiating system, the two react together *in situ* to form a stannous alkoxide, Sn(OR)$_2$, and octanoic acid, as shown in equations (4a) and (4b).

$$Sn(Oct)_2 \;+\; ROH \;\rightleftharpoons\; OctSnOR \;+\; OctH \quad (4a)$$

$$OctSnOR \;+\; ROH \;\rightleftharpoons\; Sn(OR)_2 \;+\; OctH \quad (4b)$$

As reported by Kowalski and co-workers[15-17], reactions (4a) and (4b) are reversible but gradually shift to the right as the alkoxide products are consumed in (4b) and in the polymerization reaction (5). Once formed, the final $Sn(OR)_2$ alkoxide then becomes the 'true' initiating species in the ring-opening polymerization of the cyclic ester monomer. The mechanism, now well established, is of the coordination-insertion type, as represented in equation (5).

$$ \text{(5)} $$
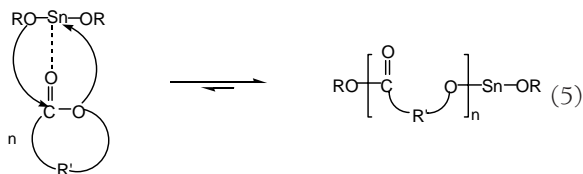
The effects of the $Sn(Oct)_2$ initiator and DEG coinitiator concentrations, as varied in this work, can now be interpreted in the light of this mechanism.

Effect of DEG Coinitiator Concentration

As seen in Table 1, as the [DEG] is decreased at constant $[Sn(Oct)_2]$, as in the Copolymer Nos. 1→5 series, the copolymer number-average molecular weight, $\overline{M}_n$, increases but with relatively little change in polydispersity (PD). These results are consistent with the findings of Kowalski and co-workers[15-17] who described the alcohol coinitiator as having a dual role. In its primary role, the alcohol reacts with $Sn(Oct)_2$ to form the $Sn(OR)_2$ initiator, as shown previously in equations (4a) and (4b). However, if the alcohol is present in a stoichiometric excess above that required to react with the $Sn(Oct)_2$, the excess alcohol can act as a chain transfer agent. This secondary role is represented in equation (6) and has the effect of terminating the growing chain by displacing the active -O-Sn-OR chain end. Even though the $Sn(OR)_2$ by-product formed is free to initiate a new chain, this chain transfer reaction increases the number of chains and thereby decreases the average molecular weight.

$$ \text{(6)} $$
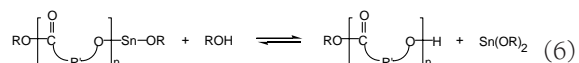
Additionally, the excess alcohol may act as a transesterification agent via alcoholysis of the ester bonds along the chain, as shown in equation (7). This would also serve to decrease the average molecular weight.

$$ \text{(7)} $$
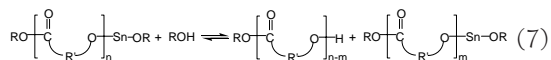
The effect of the [DEG] on molecular weight also has implications as far as the semi-crystalline morphology is concerned. As seen in Table 2 and Fig 4, as the [DEG] decreases (and $\overline{M}_n$ increases) through Copolymer Nos. 1-5, the melting transition resolves itself into two distinct ranges. These ranges obviously correspond to CL-rich and LL-rich crystalline domains, made possible by the tapered sequencing within the samples.

Effect of $Sn(Oct)_2$ Initiator Concentration

According to the previous equations (4a) and (4b), since the $Sn(Oct)_2$ initiator is the source of the active Sn-O bonds, a decrease in its concentration should result in a decrease in that of the $Sn(OR)_2$ formed. In turn, this should decrease the rate of polymerization but increase the $\overline{M}_n$ of the polymer product. In this work, a noticeable decrease in rate was observed, albeit subjectively since this was not a detailed kinetic study as such. Indeed, this was the reason why the reaction time needed to be increased from 24 to 48 hrs for $[Sn(Oct)_2] < 0.02$ mol %. However, as the results in Table 1 show, as the $[Sn(Oct)_2]$ decreased for Copolymer Nos. 6→8, an increase in $\overline{M}_n$ was not observed. Instead, remained fairly constant but with a decrease in polydispersity (PD) from 2.00→1.50.

Possible explanations for these results can be derived from the previous mechanistic considerations. For example, in this work, and typical of similar studies, a relatively large excess of the DEG coinitiator was used, well above the amount required simply to generate the $Sn(OR)_2$ alkoxide. Consequently, it is quite conceivable that the effect of the excess DEG as a chain transfer agent could have obscured the effect that the $[Sn(Oct)_2]$ would have had on $\overline{M}_n$. Another point to note here is that $Sn(Oct)_2$ is an effective transesterification catalyst. Therefore, in addition to its reaction with DEG in equation (4a), it may also have a significant role to play in facilitating the type of alcoholysis reaction shown in equation (7). This role is visualized in more detail in equation (8). Similar reactions can be envisaged for both intermolecular transesterification between different polymer chains and intramolecular transesterification (back-biting) within the same chain. These competing side-reactions will tend to obscure the effect of the $[Sn(Oct)_2]$ on $\overline{M}_n$, especially when used in conjunction with an excess of DEG.

$$\text{(8)}$$
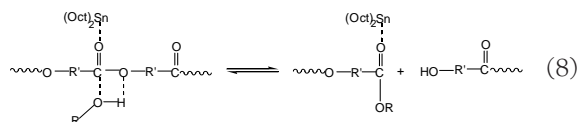
Further evidence of the contrasting effects of the $Sn(Oct)_2$ and DEG concentrations is provided by the results in Table 2. Whereas the $[Sn(Oct)_2]$ appeared to have little effect on $\overline{M}_n$ in Table 1, Table 2 shows that it had a much more noticeable effect on the comonomer sequencing. As the $[Sn(Oct)_2]$ decreased for Copolymer Nos. 6→8, the $\overline{L}_{LL}$ and $\overline{L}_C$ values increased progressively, indicating a less randomized sequencing. This would be consistent with less transesterification and also with the decreasing PD values in Table 1. Furthermore, the DSC curves in Fig 5 suggest differences in the copolymers semi-crystalline morphology, as would be expected from variations in comonomer sequencing. This combined evidence points to $Sn(Oct)_2$ having key roles to play in controlling not only the kinetics of the polymerization but also the chemical microstructure of the final product.

CONCLUSIONS

The main focus of attention in this paper has been on the effects of the $Sn(Oct)_2$ initiator and DEG coinitiator concentrations. As the results have shown, the DEG coinitiator plays a dual role: (a) to react with the $Sn(Oct)_2$ to form the 'true' alkoxide initiator and (b) to act as a chain transfer agent. It is in this latter role (b), when present in stoichiometric excess over that required for role (a), that the DEG can effectively control the molecular weight of the final copolymer. The $Sn(Oct)_2$ also appears to have a dual role. Firstly, since it is the source of the active Sn-O bonds, it exerts a rate-controlling effect. Secondly, but less obviously, the $Sn(Oct)_2$ seems to have an effect on the copolymer microstructure. As the $[Sn(Oct)_2]$ increases, the comonomer sequencing appears to become more randomized, an effect usually associated with the ability of $Sn(Oct)_2$ to act as a transesterification catalyst.

Clearly, the overall polymerization mechanism in this type of system is a complex one, comprising as it does a myriad of interdependent reversible reactions. Inevitably, this means that the 'true' $Sn(OR)_2$ initiator concentration is uncertain, thus detracting from both kinetic and microstructural control. To overcome this problem, it would seem logical to synthesize the $Sn(OR)_2$ separately and then add it directly rather than have to generate it *in situ*. However, despite this obvious advantage, $Sn(Oct)_2$ remains the popular initiator of

choice in the literature due to its commercial availability, high efficiency and, importantly as far as biomedical polymers are concerned, its status as an FDA-approved food additive. Current work in the Biomedical Polymers Technology Unit in Chiang Mai is looking at the more direct $Sn(OR)_2$ route and the results will form the subject of a future paper.

In conclusion, as interest increases in biodegradable polyesters for use in biomedical applications, so does the demand for more controlled molecular architectures. This demand can only be met through understanding the mechanism and using this understanding to achieve the necessary reaction control. Looking ahead to the future, it is likely that the development of new initiating systems will be as important as the design of new polymer architectures in this active field.

REFERENCES

1. Schindler A, Jeffcoat R, Kimmel GL, Pitt CG, Wall ME and Zweidinger R (1977) Biodegradable polymers for sustained drug delivery. In: *Contemporary Topics in Polymer Science, Vol 2* (Edited by Pearce JR and Schaefger EM), pp 251-89. Plenum, New York, USA.
2. Ge H, Hu Y, Yang S, Jiang X and Yang C (2000) Preparation, characterization and drug release behaviors of drug-loaded ε-caprolactone/L-lactide nanoparticles. *J Appl Polym Sci* **75**, 874-82
3. Nakamura T, Shimizu Y, Matsui T, Okumura N, Hyon SH and Nishiya K (1992) A novel bioabsorbable monofilament surgical suture made from (ε-caprolactone, L-lactide) copolymer. In: *Degradation Phenomena in Polymeric Materials* (Edited by Planck H, Dauner M and Renardy M), pp 153-62. Springer-Verlag, Berlin, Germany.
4. Tomihata K, Suzuki M, Oka T and Ikada Y (1998) A new resorbable monofilament suture. *Polym Degrad Stab* **59**, 13-8.
5. Den Dunnen WFA, van der Lei B, Robinson PH, Holwerda A, Pennings AJ and Schakenraad JM (1995) Biological performance of a degradable poly(lactic acid -ε-caprolactone) nerve guide: Influence of tube dimensions. *J Biomed Mater Res* **29**, 757-66.
6. Grijpma DW, Zondervan GJ and Pennings AJ (1991) High molecular weight copolymers of L-lactide and ε-caprolactone as biodegradable elastomeric implant materials. *Polym Bull*

25, 327-33.

7. Grijpma DW and Pennings AJ (1991) Polymerization temperature effects on the properties of L-lactide and ε-caprolactone copolymers. *Polym Bull* **25**, 335-41.

8. Choi EJ, Park JK and Chang HN (1994) Effect of polymerization catalysts on the microstructure of P(LLA-*co*-εCL). *J Polym Sci, Part B: Polym Phys Edn* **32**, 2481-9.

9. Hiljanen-Vainio M, Karjalainen T and Seppälä J (1996) Biodegradable lactone copolymers. I : Characterisation and mechanical behaviour of ε-caprolactone and lactide copolymers. *J Appl Polym Sci* **59**, 1281-8.

10. In't Veld PJA, Velner EM, Van De Witte P, Hambuis J, Dijkstra PJ and Feijen J (1997) Melt block copolymerization of ε-caprolactone and L-lactide. *J Polym Sci, Part A: Polym Chem Edn* **35**, 219-26.

11. Vanhoorne P, Dubois Ph, Jerome R and Teyssie Ph (1992) Macromolecular engineering of polylactones. 7: Structural analysis of copolyesters of ε-caprolactone and L- or D,L-lactide initiated by Al(Oi-Pr)₃. *Macromolecules* **25**, 37-44.

12. Albertsson A-C and Varma IK (2003) Recent developments in ring-opening polymerization of lactones for biomedical applications. *Biomacromolecules* **4**, 1466-86.

13. Tsuji H, Mizuno A and Ikada Y (2000) Enhanced crystallization of poly(L-lactide-*co*-ε-caprolactone) during storage at room temperature. *J Appl Polym Sci* **76**, 947-53.

14. Perrin DE and English JP (1997) In: *Handbook of Biodegradable Polymers* (Edited by Domb AJ, Kost J and Wiseman DM), Chap 1 (Polyglycolide and Polylactide) pp 3-27, and Chap 3 (Polycaprolactone), pp 63-77, Harwood Academic Publishers, Amsterdam, Netherlands.

15. Kowalski A, Duda A and Penczek S (2000) Mechanism of cyclic ester polymerization initiated with tin(II) octoate. 2: Macromolecules fitted with tin(II) alkoxide species observed directly in MALDI-TOF spectra. *Macromolecules* **33**, 689-95.

16. Kowalski A, Libiszowski J, Duda A and Penczek S (2000) Polymerization of L,L-dilactide initiated by tin(II) butoxide. *Macromolecules* **33**, 1964-71.

17. Kowalski A, Duda A and Penczek S (2000) Kinetics and mechanism of cyclic esters polymerization initiated with tin(II) octoate. 3: Polymerization of L,L-dilactide. *Macromolecules* **33**, 7359-70.